DOI: 10.1002/chem.200700321

# Functional Organogel Based on a Salicylideneaniline Derivative with Enhanced Fluorescence Emission and Photochromism

**Pengchong Xue,[a, b] Ran Lu,*[a] Guojun Chen,[a] Yuan Zhang,[c] Hiroyuki Nomoto,[b] Makoto Takafuji,[b] and Hirotaka Ihara*[b]**

**Abstract:** A new organogelator based on a salicylideneaniline derivative with cholesterol moieties was synthesized, and it was proposed that it could gelate various organic solvents, such as 1-butanol, 1-octanol, butyl acetate, tetrachloromethane, benzene, toluene through combination with a gelation test. From the results of analysis by UV/Vis absorption, circular dichroism (CD), X-ray diffraction (XRD), scanning electron microscopy (SEM), and transmission electron microscopy (TEM) studies and semiempirical (AM1) calculations, we believed that the gelator molecules could self-assemble into left-handed helical nanofibers through unimolecular layer packing, which further twisted into the thicker fibers and constructed 3D networks in the gel phase. Interestingly, the organogel exhibited strong fluorescence enhancement relative to a solution of the same concentration because of the formation of J aggregations. Meanwhile, photochromism of the organogel could take place under UV-light irradiation. Both strong fluorescence emission and photochromism properties were concurrent in one system based on a salicylideneaniline derivative. It was suggested that the self-assembly of the functional organogelator could lead to unique photophysical properties.

**Keywords:** fluorescence · helical structures · photochromism · self-assembly

## Introduction

Recently, low-molecular-mass gelators (LMMGs), especially with functional and chiral moieties, have attracted substantial attention in supramolecular chemistry and materials science[1] because some of their physical properties can be modulated during the formation of the gels, in which the gelator molecules self-assemble into nanoscale superstructures, such as fibers, rods, and ribbons, through weak noncovalent interactions (i.e., hydrogen bonding, π–π, van der Waals, coordination, and charge-transfer interactions). So far many functional modules have been successfully integrated into LMMGs, which have specific applications in light harvesting;[2] energy and charge transfer;[3] photo, enzyme, and other switches;[4] and chiral or molecular-shape selection.[5] It is well known that salicylideneaniline derivatives could exhibit unusual functionalities, such as tunable fluorescence,[6] photochromism,[7] thermochromism,[8] solvatochromism,[9] liquid crystals,[10] and nonlinear optics.[11] To date, no example of an organogelator that consists of a salicylideneaniline moiety has been reported.

As suggested by van Esch and Feringa,[1b] if an organic compound is expected to be a gelator for an organic solvent three important guidelines must be followed: 1) strong self-complementary and unidirectional intermolecular interactions to induce one-dimensional (1D) packing of the molecules need to be present; 2) control of the interfacial energy between the aggregation and the solvent to adjust the solubility of the gelator and to prevent crystallization is required; and 3) some factors that favor the cross-linking of 1D fibers to form 3D networks should be considered. Recently, Birkedal and Pattison reported the crystal structure of bis(4-[salicylideneamino]phenyl)methane (**1′**),[12] which

[a] Dr. P. Xue, Prof. R. Lu, G. Chen
Key Laboratory for Supramolecular Structure and Materials
Ministry of Education, College of Chemistry
Jilin University, Changchun, 130012 (China)
Fax: (+86) 431-8892-3907
E-mail: luran@mail.jlu.edu.cn

[b] Dr. P. Xue, H. Nomoto, M. Takafuji, Prof. H. Ihara
Department of Applied Chemistry and Biochemistry
Kumamoto University, 2-39-1 Kurokami
Kumamoto 860–8555 (Japan)
Fax: (+81) 092-342-3662
E-mail: ihara@kumamoto-u.ac.jp

[c] Dr. Y. Zhang
State Key Laboratory of Theoretical and Computational Chemistry
Institute of Theoretical Chemistry
Jilin University, Changchun, 130012 (China)

Supporting information for this article is available on the WWW under http://www.chemeurj.org/ or from the author.

  

has a V-shaped conformation and packs into 1D J aggregations along the *b* axis through strong π–π interactions among the aromatic rings (Figure 1). Such close stacking

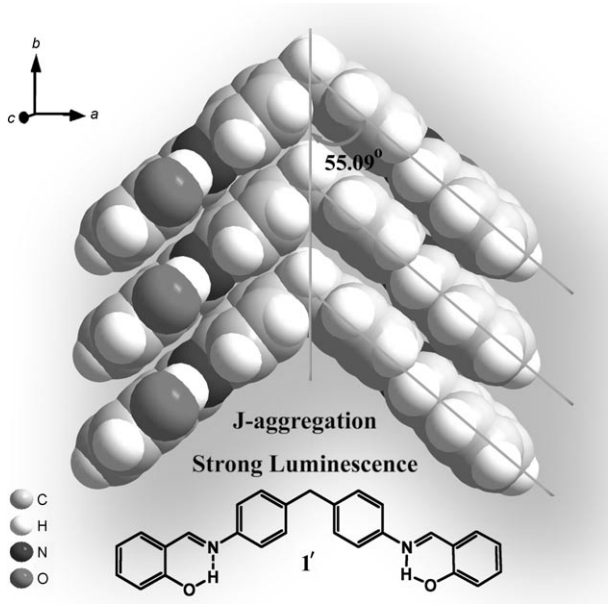


Figure 1. One-dimensional packing of **1′** along the *b* axis in the crystal state.

(the distance between the two adjacent parallel aromatic rings is 3.6 Å) of the salicylideneaniline groups leads to enhanced photoluminescence and non-photochromism under UV-light irradiation.[7e,13] Therefore, if such Schiff base dimer is integrated into the designed molecule, it would possibly self-assemble and be arranged into 1D aggregations through unidirectional π–π interactions between the aromatic rings. On the other hand, the chiral group in the gelator is usually considered to be an important factor to prevent crystallization from the solvent;[1c] therefore, many gelators with cholesterol units have been reported.[14]

Herein, we present the synthesis and characterization of **1**, composed of cholesterol and salicylideaniline moieties (Scheme 1), which is a good gelator in various organic solvents. Investigation of the self-assembly properties of the gelator revealed that **1** could form left-handed helical nanofibers through unimolecular layer packing, which further constructed 3D networks in the organogel. Interestingly, the fluorescence emission intensity of the organogel was more than 1000 times higher than that of the solution at the same concentration as a result of the formation of J aggregation in the gel state. Meanwhile, under UV-light irradiation, the photochromism of the organogel could be observed. The appearance of both strong fluorescence emission and photochromism in the salicylideneaniline derivative has rarely been reported because the strong photoluminescence is consistent with the dense stacking of molecules, which strongly suppresses photoinduced isomerization. This behavior suggests that the introduction of certain aliphatic moieties into

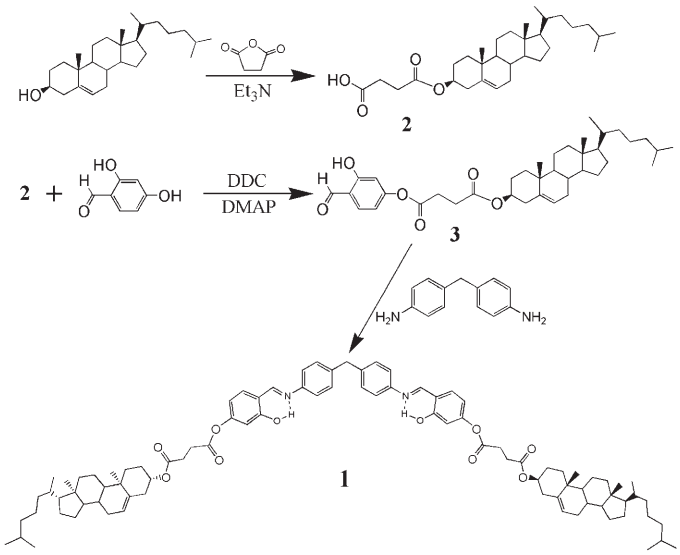


Scheme 1. The synthetic route to organogelator **1**. DCC = dicyclohexyl carbodiimide, DMAP = *N*,*N*-dimethyl-1,3-propanediamine.

the functional organogelators may result in unusual optical properties as a result of adjusting the weak intermolecular interactions, thus leading to supramolecular self-assemblies with special superstructures.

## Results and Discussion

**Gelation behavior:** A series of organic solvents was employed to reveal the gelation behavior of **1** (Table 1). Compound **1** readily dissolves in chloroform, dichloromethane, and THF at room temperature, but was insoluble in lower alcohols and esters, such as ethanol and ethyl acetate, and aliphatic hydrocarbon solvents, such as cyclohexane, *n*-hexane, and *n*-decane, even with heating. Compound **1** can also gelatinize some higher alcohols and esters and some nonpolar aromatic solvents, including 1-butanol, 1-octanol, butyl acetate, tetrachloromethane, benzene, and toluene. However, the minimum gelation concentration (MGC) necessary for gel formation in benzene and toluene is relatively large (MGC > 0.5 wt vol %$^{-1}$) compared to that in 1-butanol,

Table 1. Gelation properties of **1** in organic solvents.[a]

| Solvent | **1**[b] | Solvent | **1**[b] |
|---|---|---|---|
| $CHCl_3$ | S | benzene[c] | G |
| $CH_2Cl_2$ | S | toluene[c] | G |
| THF | S | cyclohexane | I |
| ethanol | I | *n*-hexane | I |
| 1-butanol | G | *n*-decane | I |
| 1-octanol | G | benzene/cyclohexane[d] | G |
| ethyl acetate | I | benzene/*n*-hexane[d] | G |
| butyl acetate | G | tetrachloromethane | G |

[a] G: stable gel formed at room temperature; S: soluble; I: insoluble. [b] Gelator = 1.0 wt vol %$^{-1}$. [c] MGC is above 0.5 wt/vol %. [d] v/v = 1:4; MGC < 0.1 wt/vol %.

  

1-octanol, butyl acetate, and tetrachloromethane (MGC $<0.2$ wt vol% $^{-1}$). The addition of cyclohexane or *n*-hexane, in which **1** is poorly soluble, into the benzene or toluene systems could decrease the MGC. For example, the system may maintain the gel state below 0.1 wt/vol% in a mixture of benzene and cyclohexane (v/v 1:4). In this case, the solvents with poor solubility for the organogelator are deemed to be the trapped solvent to decrease the MGC.[15] As a result, **1** is an effective gelator for various organic solvents.

**UV/Vis absorption and circular dichroism (CD) spectra**: Variable-temperature absorption spectra of **1** in benzene/cyclohexane and 1-butanol systems were investigated to monitor the interactions between the chromophores, the salicylideneaniline moieties, during the formation of the gels (Figure 2). The absorption intensities of gels at lower temperatures are weaker than those at higher temperatures, thus promoting the interactions between the chromophores.[16] Moreover, relative to the solutions, a red-shift of

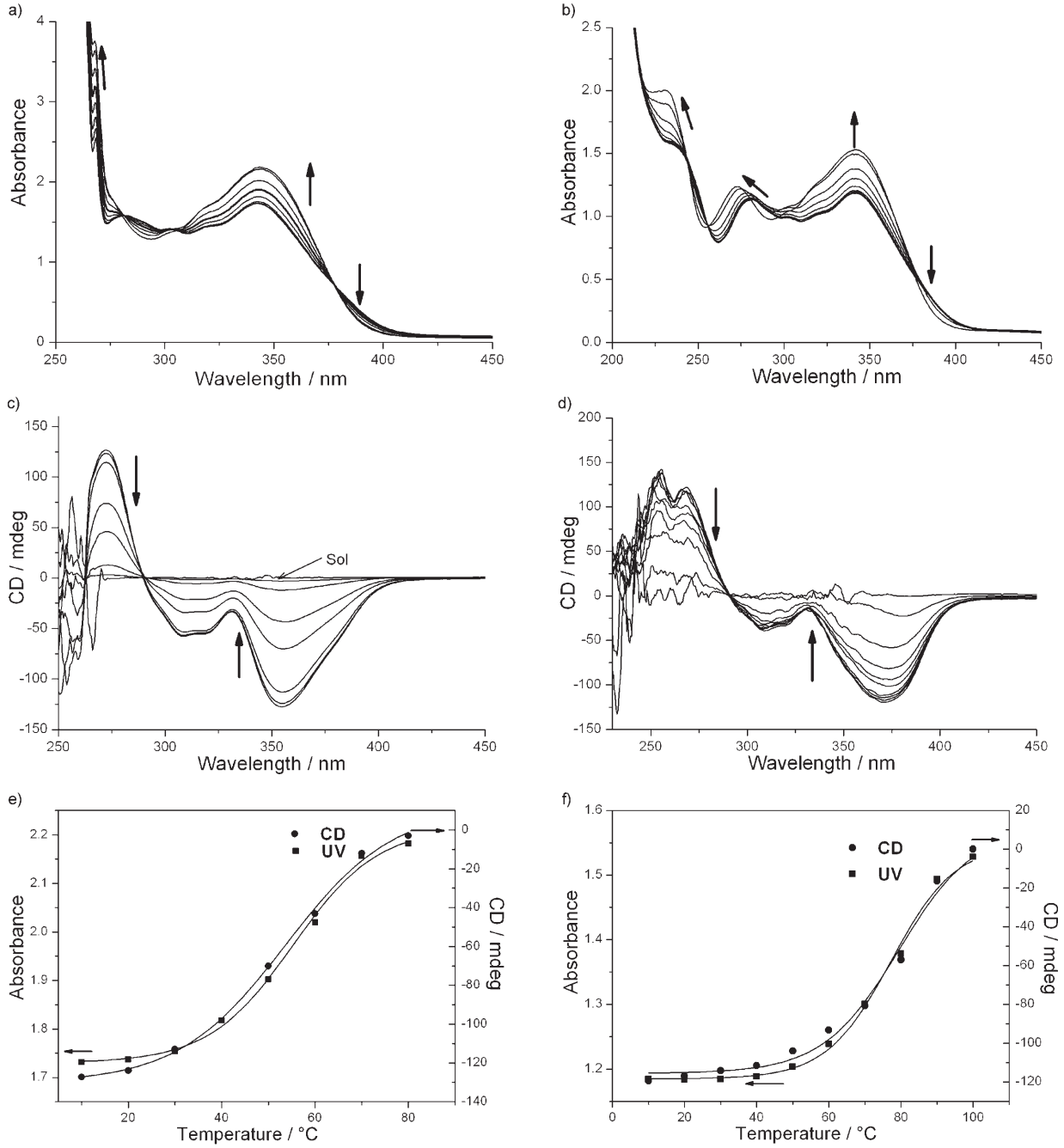


Figure 2. Temperature-dependence of the UV/Vis (a and b) and CD spectra (c and d) of the benzene/cyclohexane and 1-butanol organogels, respectively. The solution of organogel in benzene at 0.1 wt vol% $^{-1}$ does not give a CD response (see the curve of the center one labeled as "sol 20 °C" in (c)). e) The plot of the absorbance and intensity of CD at 343 and 354 nm, respectively, for the benzene/cyclohexane gel as a function of the temperature. f) The plot of the absorbance and intensity of CD at 343 and 370 nm, respectively, for the 1-butanol gel. The concentrations in all cases are 0.1 wt/vol%.

  

2 nm can be detected for the two gels, thus indicating the formation of J aggregations of salicylideneaniline in the gel state.[17] However, the maximum absorption peak of **1′** at 346 nm in dilute solution shifts to 360 nm in the crystal state, and such a large red-shift ($\Delta\lambda = 14$ nm; see the Supporting Information) shows one strong exciton coupling attributed to the close distance between the chromophores in the crystal. The small red-shift phenomenon in the gel phase suggests that the exciton coupling of the chromophores is weaker and that the distance between the chromophores is larger than that in **1′** in the crystal state.[18] It is believed that the large cholesterol group actually inhibits the closeness of the chromophores (as will be discussed further later on). The "melting" temperatures were calculated from Figure 2e,f for the phase transitions from aggregation to molecularly dissolved species, not from gel to sol.[19] There is a clear dependence of the aggregation melting transition on the solvent; for example, the melting transition increases from 55 °C for the benzene/cyclohexane gel to 77 °C for the 1-butanol gel at the same concentration.

CD spectroscopy is considered a powerful tool in the study of the assembly processes that lead to the helical superstructures. In the CD spectra, both gels give similar signals and non-bisignate exciton couplets with the opposite signals, thus indicating no central helical overlay between the dipole moments of the two gelators in the gels[20] (Figure 2c,d). Measurement of molar ellipticity ($[\theta] = -175\,000$ and $-164\,144$ deg cm$^2$ dmol$^{-1}$ for benzene/cyclohexane and 1-butanol, respectively) reveals a similar intensity of exciton coupling for both gels. Combined with the results of the UV/Vis absorption spectra, it is rational that **1** is packed in an anticlockwise helical direction in both gel phases.[21] In addition, the melting transitions obtained from temperature-dependent CD spectra were the same as those from the observation by UV/Vis spectroscopy (Figure 2e,f).

**Variable-temperature $^1$H NMR spectra:** The NMR spectra can reveal the interactions not only between the chromophores but also between the cholesterol moieties. The temperature-dependent $^1$H NMR spectral changes in **1** in a [$D_6$]benzene/[$D_{12}$]cyclohexane gel and the assignment of the key peaks for the aromatic and aliphatic (cholesterol and succinic ester) subunits is shown in Figure 3. The peaks ascribed to the aliphatic moieties are consistently visible at 30–90 °C and become gradually sharper and stronger with increasing temperature.[22] On the other hand, weak and broad NMR resonance peaks for the aromatic units can only be found over 50 °C. It is well known that the broadening and decrease in the intensity of the NMR resonance peaks can be interpreted as an indication of restricted freedom of motion, such as the behavior in the solid state. Therefore, the aromatic moieties behave "solid-like" and exhibit a relatively rigid structure compared to the aliphatic units. This behavior also suggests that the salicylideneaniline moiety has a poorer solubility than the cholesterol groups in the gel phase.[23] Moreover, the peak at $\delta = 12.9$ ppm illustrates that **1** exists as a *trans*-enol form (*E*-OH form) even

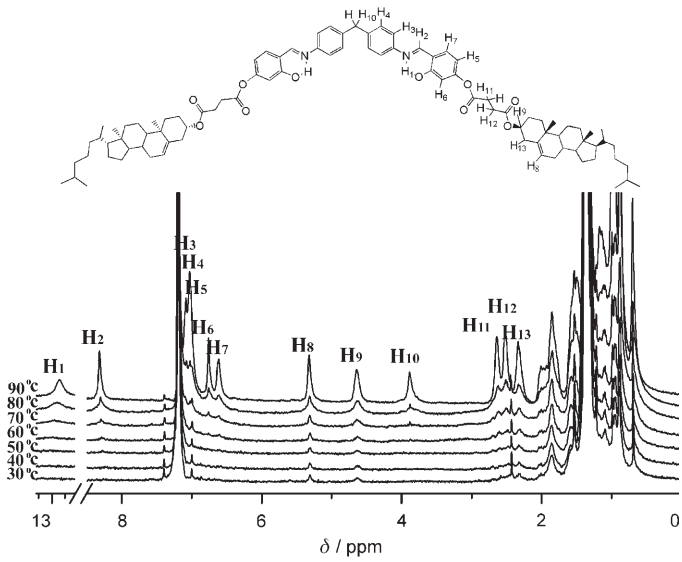


Figure 3. Temperature-dependent $^1$H NMR spectra of the [$D_6$]benzene/[$D_{12}$]cyclohexane organogel **1** at 0.2 wt/vol %.

at high temperature;[24] this result can be further confirmed by the FT-IR spectrum, as no N–H vibration band at around 3310 cm$^{-1}$ was found and a strong C=N band at 1622 cm$^{-1}$ appeared.

**Small-angle X-ray diffraction investigations (SAXD):** The measurement of the SAXD of the gel can provide information about the long-range regulation of the molecular self-assembly, thereby the packing model of molecules in the gel phase can be supposed. Figure 4 shows the SAXD spectrum of the xerogel obtained from the benzene/cyclohexane gel. The good diffraction pattern was characterized by three reflection peaks of 5.81, 2.91 and 1.93 nm, which were exactly in the ratio of 1:$^1/_2$:$^1/_3$, thus indicating a lamellar organization within the aggregates of gel **1** with an interlayer distance of 5.81 nm.[25]

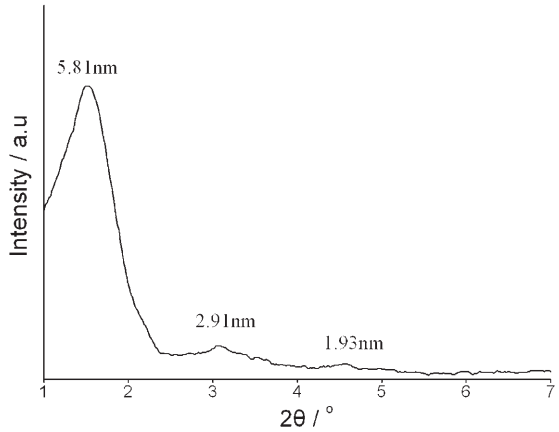


Figure 4. Small-angle XRD diagram of the xerogel **1** obtained from the benzene/cyclohexane gel.

  

**Transmission electron microscopy (TEM) and scanning electron microscopy (SEM) investigations:** SEM and TEM images of the 1-butanol (polar solvent) and benzene/cyclohexane (nonpolar solvent) gels were obtained to study the microstructures of the organogels and the molecular self-assembly properties. A SEM image of the benzene/cyclohexane gel shows that many nanofibers 30–70 nm in width and tens of micrometers in length form the basis of the 3D networks so that the flow of the solvent can be prevented to induce the formation of a solid-like gel (see Figure 5a). Moreover, the TEM image of the benzene/cyclohexane gel shows lots of helical nanofibers. On careful examination, we found that these fibers are all left-handed helices and the diameter of the thinnest fibers is about 5.8 nm, which is in agreement with the periodicity of the structure (5.81 nm) suggested by the XRD studies (Figure 5b). Furthermore, we also found that two or more fibers 5.8 nm in diameter twist around each other to form larger fibers with diameters of 11.6, 17.4, and 24.8 nm, thus further confirming the evidence of the layer structure. Moreover, the helical pitch of the twisted fiber is independent of the diameter of the fiber, and all the fibers have similar helical pitches of 45 nm. Similar to the benzene/cyclohexane gel, some left-handed helical fibers with diameters of 5.8 nm and helical pitches of approximately 50 nm were observed in the 1-butanol gel (Figure 5c). It was thought that the microstructures of the molecular self-assemblies in both gels are similar.

**Molecular packing model**: Semiempirical (AM1) calculations were performed to optimize the ground-state geometry of **1** to reveal the molecular packing model. The results show that **1** has a V-shaped conformation (Figure 6a), which coincides with that of **1′**. The molecular length for the extended form is estimated to be 5.78 nm, which is in accordance with the long period of the lamellar structure in the gel phase. As the results of the UV/Vis spectra indicated that the aromatic moieties formed J aggregations with weak exciton coupling, it can be confirmed that the gelator molecules are arranged in parallel along the growth direction of the fiber and are further extended to form a 1D fibrous structure. In this model, the distance between two parallel salicylideneaniline moieties reaches up to 5.0 Å, longer than that of **1′** (3.6 Å) in the crystal state because of the effect of the spatial hindrance of the cholesterol group (Figure 6b). In addition, the CD spectra and TEM observations suggest that the molecules are packed in an anticlockwise direction. Therefore, the molecular packing model in the gel phase

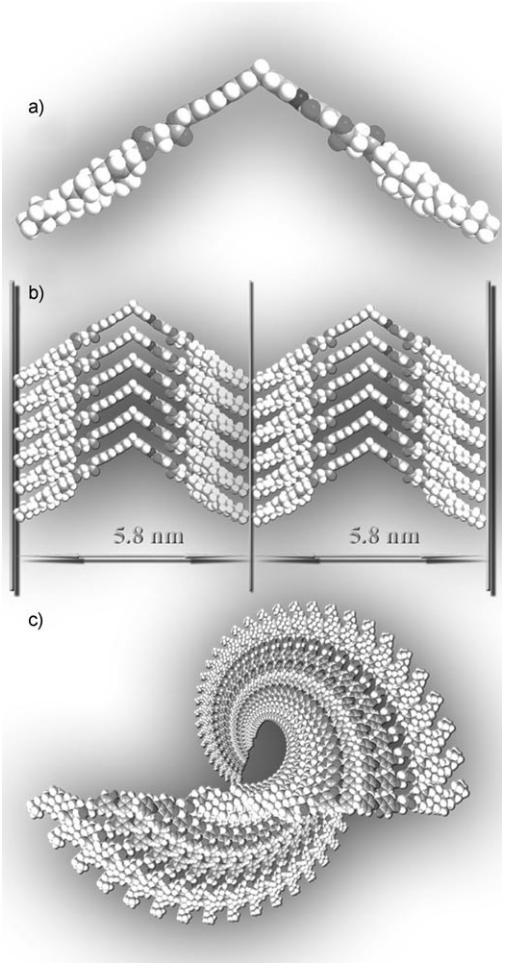


Figure 6. a) The optimized structure of **1** through the AM1 quantum mechanical calculations. b) Schematic illustration of the monomolecular layer structure with a period distance of 5.8 nm in the gel state. c) Bimolecular helical packing along the direction of the long axis.

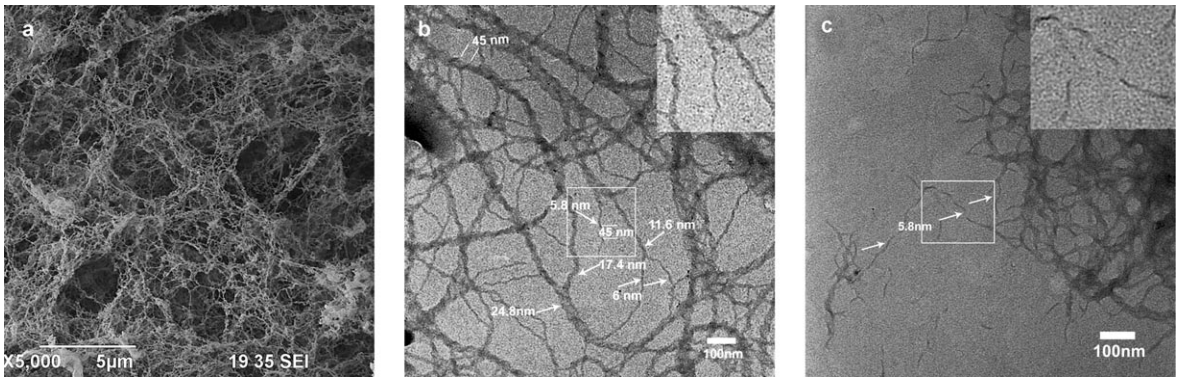


Figure 5. SEM image of the benzene/cyclohexane gel (a) and the TEM images of the benzene/cyclohexane (b) and 1-butanol (c) gels.

  

can be illustrated as shown in Figure 6c. Considering the helical pitch (namely, 450 and 500 Å for the benzene/cyclohexane and 1-butanol gels, respectively), it can be deduced that the fiber within a helical pitch includes approximately 90 molecules in the benzene/cyclohexane gel and 100 molecules in the 1-butanol gel, and that the torsion angles of adjacent two molecules in both gels are 4 and 3.6°, respectively.

**Enhanced fluorescence emission from sol to gel**: In general, after the *E*-OH form of salicylideneaniline in the ground state absorbs one photon, the excited-state intramolecular rapid proton-transfer process from the oxygen to the nitrogen atom occurs and yields the excited-state *Z*-NH form owing to the lower potential energy.[26] Moreover, the *Z*-NH form can undergo a torsion and transform into a photochromic product (i.e., the *E*-NH form) if there is enough space to permit the molecule to rotate, as reported by Kawato and co-workers,[7d] or it can undergo a transition from the excited state to the ground state accompanied by a longer emission wavelength[6a] and then return to the *E*-OH ground state rapidly. Therefore, the behavior of the *Z*-NH form can lead to a large Stokes shift relative to the absorption peak in the *E*-OH form. The detailed photoinduced isomerization and photoluminescence processes are shown in Scheme 2.

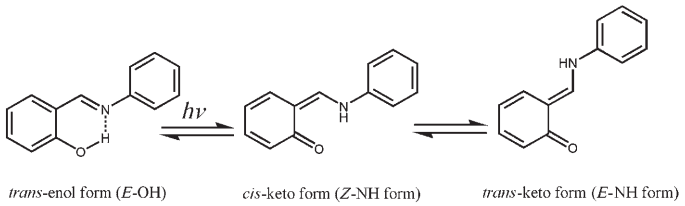


Scheme 2. Photoinduced isomerization and photoluminescence processes of a typical salicylideneaniline moiety.

Under UV-light irradiation, the benzene/cyclohexane and 1-butanol gels emit strong green fluorescence, which gradually decreases as the temperature increases (Figure 7). The maximum emission peaks of both gels are located at 520 nm, and a large Stokes shift (177 nm) is observed relative to the absorption of the gels. Interestingly, at the same concentration as the benzene/cyclohexane gel, a solution of **1** in benzene, in which the molecules are confirmed to exist in the unimolecular isolated state because no CD signal is detected (Figure 2c), gives very weak fluorescence emission ($\Phi_f = 2.31 \times 10^{-5}$); furthermore, the fluorescence intensity increases gradually when cyclohexane is continually added into the solution of **1** in benzene to induce the formation of the self-assembly of **1**. When the volume ratio of cyclohexane to benzene reaches 4:1, the fluorescence quantum yield of the system reaches 0.0241, which is the same as that of the gel and more than 1000 times greater than that of the solution of **1** in benzene. These results suggest that the enhanced fluorescence emission of the gel is caused by the formation of molecular aggregations.

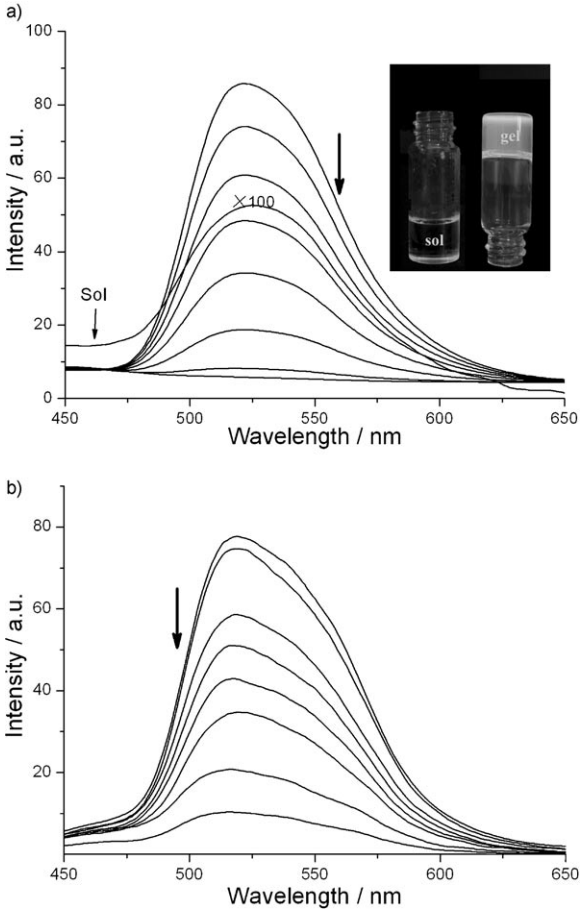


Figure 7. Temperature-dependence of the fluorescence emission of the benzene/cyclohexane (a) and 1-butanol (b) gels. Inset: photograph of the benzene/cyclohexane gel and benzene sol at 0.1 wt/vol irradiated by 365-nm light.

In recent years, a few samples with enhanced emission induced by molecular aggregation have been reported; for example, Tang and co-workers reported a pentaphenylsilole derivative with enhanced emission after aggregation[27] and suggested that the enhanced fluorescence can be explained by the planar conformation in the solid state, which can activate the radiation process.[28] Herein, in respect to the absorption band of the gel with only a small red-shift of 2 nm relative to that in solution, the contribution of the molecular planarization to the enhanced emission is not taken into account. It is well known that an increase in the rigidity of a molecule can decrease molecular vibrations, probably suppress the internal conversion of an excited molecule, and may increase the fluorescence quantum yield.[29] In addition, the fluorescence intensity of the π-conjugated chromophores is correlated with the π aggregation, such as H and J aggregations.[30] H aggregations, in which the molecules are aligned in parallel to each other in a head-to-head form, tend to increase the internal conversion from a higher electronic state into a lower one so that the fluorescence emis-

  

sion is effectively quenched. In contrast, the molecules are arranged into a head-to-tail stack as in J aggregation, in which the transition from the lower couple excited state of the molecule to the ground state is allowed; as a result, the absorption peak will red-shift and the fluorescence emission will be stronger than that of the monomer.[31] In our case, the gelator molecules form J aggregations and cross-link into a solid-like 3D network in the gel phase, so the enhanced emission of the gel is attributed to the synergetic effect of the restricted molecular motion and the formation of J aggregations.

Time-resolved fluorescence spectra were measured to obtain further information about the excited state of **1**. Both the monomer solution and gel gave double-exponential decay with average lifetimes of 6.98 and 5.78 ns, respectively (Figure 8). According to the equations $\tau^{-1}=k_r+k_{nr}$ and $k_r=$

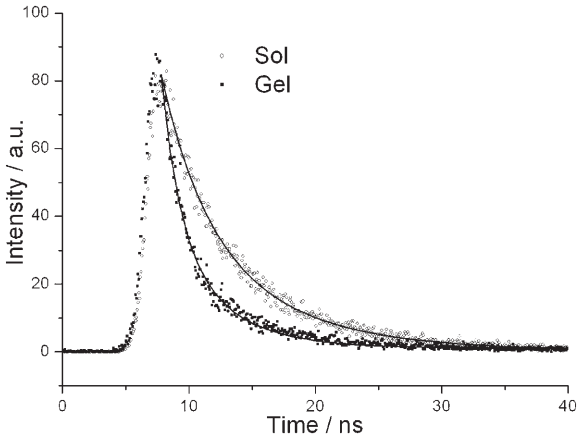


Figure 8. Fluorescence decay of the benzene/cyclohexane gel and the benzene sol at 20 °C and $\lambda_{em}=520$ nm.

$\Phi_f/\tau$, the radiative rate constant $k_r$ and total nonradiative rate constant $k_{nr}$ of **1** in the monomer and J aggregation state were calculated (Table 2). Although $k_{nr}$ increases slightly as a result of the formation of the gel, thus suppressing the fluorescence emission, efficient radiative transition increased more than 1000 times. Therefore, the aggregation-induced fluorescence enhancement is mainly ascribed to the increase in the value of $k_r$.

Table 2. The fluorescence quantum yields and the radiative and total nonradiative rates of the benzene sol and the benzene/cyclohexane gel.

| | $\Phi_f$ [$10^{-2}$] | $\tau_1$ [ns] | $\tau_2$ [ns] | $<\tau>$ | $k_r$ [$10^6$ s$^{-1}$] | $k_{nr}$ [$10^8$ s$^{-1}$] |
|---|---|---|---|---|---|---|
| benzene sol | 0.0023 | 3.43 | 8.65 | 6.98 | 0.0033 | 1.43 |
| benzene/cyclohexane gel | 2.41 | 1.92 | 9.44 | 5.78 | 4.15 | 1.69 |

**Photochromism and photoinduced transition from gel to sol**: As deduced from the 3D X-ray structures, the crystals based on salicylideneaniline exhibit two mutually exclusive properties: either thermochromism or photochromism.[7e,32] In the thermochromic crystal, the molecules are planar and close-packed through π–π interactions so that strong fluorescence emission can be detected, such as in **1′**. On the contrary, in the photochromic crystals there is large dihedral angle between the planar salicylaldimine group and the aniline ring, thus inducing an open crystal structure with incompact molecular packing.

From the above discussion, **1** can undergo regular aggregation and emit strong fluorescence in the gel phase, whose properties are similar to those of the thermochromic crystal. However, the UV/Vis absorption spectra and molecular packing model illustrated that the packing of the Schiff base group was not very tight, and the temperature-dependent $^1$H NMR spectra suggested that the cholesterol groups possessed significant freedom of motion. Therefore, it was worth investigating whether the photochromism of the organogel could take place under UV irradiation. Figure 9 shows

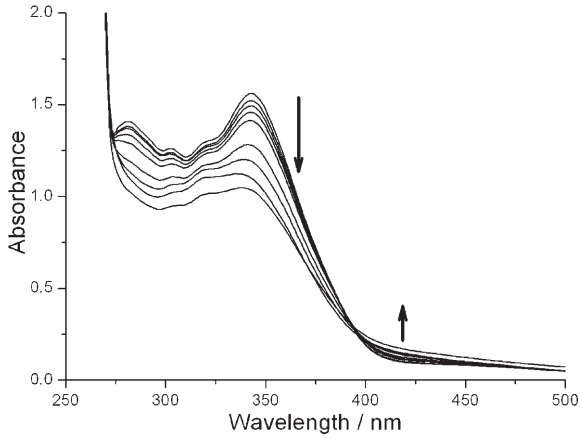


Figure 9. Changes in the UV/Vis absorption spectra of the benzene/cyclohexane gel with irradiation time under 365-nm light from a high-pressure mercury lamp. Inset: the plot of the absorbance at 343 nm as a function of the irradiation time.

the absorption spectral change of the benzene/cyclohexane gel with the irradiation time. After irradiation with 365-nm light, the band at 343 nm decreased and a new peak appeared at 450 nm, which could intensify when the irradiation time was prolonged.[33] On the other hand, the FT-IR spectrum of the sample after irradiation revealed two new peaks at 3326 and 1660 cm$^{-1}$, ascribed to NH and α,β-unsaturated ketone vibration absorptions, respectively (see the Supporting Information). This spectrum suggests that **1** shows significant photochromic properties in the gel phase, although it also exhibits emission enhancement as a thermochromic crystal, which is quite different from the traditional photochromic salicylideneaniline with non-fluorescence. Moreover, after being irradiated for 110 min, the gel state transformed into a solution, although not all molecules existed in the keto form.

  

## Conclusion

In summary, a new organogelator based on a salicylideneaniline derivative with cholesterol units was synthesized, which could gel various organic solvents. SEM and TEM images revealed that the gelator molecules self-assembled into 1D helical fibers with diameters of approximately 5.8 nm in an anticlockwise direction, which further twisted into thicker fibers and constructed 3D networks. Through combining the results of the UV/Vis spectra, CD spectra, and semiempirical (AM1) calculations, the molecular packing model in the gel phase was illustrated. Interestingly, the fluorescence emission intensity of the organogel was more than 1000 times higher than that of the solution at the same concentration as a result of the formation of J aggregations and the restricted molecular motion in the gel state. Meanwhile, the UV irradiation could induce the isomerization of salicylideneaniline in the organogel because of the large cholesterol group, thus resulting in a loose packing of the molecules and permitting the molecule to rotate. Strong fluorescence emission and photochromism could be involved in such a gel system based on a salicylideneaniline derivative, thus indicating that the expected optical properties may be realized through tuning the self-assembly process of the functional gelator.

## Experimental Section

**Instruments**: The IR spectra were measured on a Nicolet-360 FT-IR spectrometer by incorporating the samples in KBr disks. The $^1$H NMR spectra were recorded on a Varian-300 EX spectrometer. The temperature-dependent $^1$H NMR spectra were measured on JEOL FX-400 spectrometer, and the NMR tube containing **1** in solvent was sealed before measurement. The SEM images were obtained using a JEOL JEM-5310 LV spectrometer. The CD spectra were recorded on JACSO J-725 spectropolarimeter. The UV/Vis spectra were determined on a Shimadzu-1601 spectrophotometer. Microanalysis was performed on a Perkin–Elmer 240C elemental analyzer. The photoluminescence measurements were taken on a JACSO PL-5600 spectrofluorometer.[34]

**TEM investigation**: A piece of the gel **1** was placed on a carbon-coated copper grid (400 mesh) followed by naturally evaporating the solvent. The TEM specimens were examined with a Hitachi mode H600 A-2 apparatus with an accelerating voltage of 100 kV.

**Gelation test of organic fluids**: The solution of gelator **1** (pre-weighed) in organic solvent was heated in a sealed test tube (diameter = 1 cm) in an oil bath until the solid was dissolved. The solution was allowed to stand at room temperature for 6 h, and the state of the mixture was evaluated by the "stable to inversion of a test tube" method.

**XRD studies:** Diffraction patterns were carried out on a Rigaku D/max-rA X-ray diffractometer with graphite-monochromated $Cu_{K\alpha}$ radiation ($\lambda = 1.5418$ Å). The accelerating voltage was set at 50 kV, with 100-mA fluxes at a scanning rate of 0.02 deg s$^{-1}$ in the $2\theta$ range of 1–10°. The XRD patterns of xerogel were obtained by casting wet gel samples in a glass flask followed by evaporation of the solvent naturally.

**Photochromism**: Preweighed **1** was added into a quartz cell and a mixture of benzene and cyclohexane (v/v 1:4) was injected into the cell. After the solid was dissolved by heating, the system was cooled to room temperature and the gel formed. A high-pressure mercury lamp was used as the irradiation-light source with a filter plate ($\lambda_{max} = 365$ nm). After irradiation for the expected time, the absorption peak was recorded on a Shimadzu-1601 spectrophotometer. The cell was maintained at 20 °C during the irradiation.

**Synthesis of the organogelator**

*3-Cholesteryloxycarbonylpropanoic acid (**2**)*: Compound **2** was synthesized according to a previously reported method.[35] A solution of cholesterol (3.87 g, 10 mmol), succinic anhydride (1.00 g, 10 mmol), and triethylamine (1.10 g, 10 mmol) in dry acetone (60 mL) was heated to reflux for 24 h. The acetone was evaporated and the resulting precipitate was recrystallized twice from glacial acetic acid. Yield: 65 %; m.p. 177.0–179.0 °C (177.0–179.0 °C in reference [34]); IR (KBr): $\tilde{\nu} = 1728$ (ester carbonyl), 1709 (acid carbonyl), 3440 cm$^{-1}$ (hydroxy); elemental analysis (%) calcd for $C_{31}H_{50}O_4$: C 76.50, H 10.27; found: C 76.01, H 10.10.

*2-Hydroxy-4-(3-cholesteryloxycarbonylpropionyloxy)benzaldehyde (**3**)*: Compound **2** (2.50 g, 5.1 mmol) and 2,4-dihydroxylbenzaldehyde (0.9 g, 6.5 mmol) were dissolved in dry $CH_2Cl_2$ (30 mL) containing pyridine (1.8 mL). The solution was cooled to 0 °C and a small amount of DMAP and DCC (2.50 g, 10 mmol) was added. The mixture was stirred for 4 h at 0–5 °C and left for 24 h at room temperature. A white precipitate was removed by filtration. After the solvent was evaporated under reduced pressure, the resultant residue was purified by column chromatography on silica gel (cyclohexane/ethyl acetate 5:1). Yield: 38 %; m.p 99.0–100.0 °C; IR (KBr): $\tilde{\nu} = 3327$ (hydroxy), 1770 and 1737 (ester carbonyl), 1661 cm$^{-1}$ (aldehyde carbonyl); elemental analysis (%) calcd for $C_{38}H_{54}O_6$: C 75.21, H 8.97; found: C 75.10, H 8.86; $^1$H NMR (300 MHz, TMS, $CDCl_3$): $\delta = 10.24$ (s, 1H), 7.60 (d, $J = 2.2$ Hz, 1H), 6.81 (d, $J = 2.2$ Hz, 1H), 6.74 (s, 1H), 5.37 (d, $J = 4.2$ Hz, 1H), 4.68 (m, 1H), 2.87 (t, $J = 7.2$ Hz, 2H), 2.72 (t, $J = 7.2$ Hz, 2H), 2.33 (t, $J = 7.2$ Hz, 2H), 2.20–1.5 ppm (m, 41H).

*4,4′-Di(2-hydroxy-4-[3-cholesteryloxycarbonylpropionyloxy]benzylideneamino)diphenylmethane (**1**)*: A solution of **3** (0.606 g, 1.0 mmol) and 4,4′-diaminodiphenylmethane (0.099 g, 0.5 mmol) in ethanol (10 mL) was heated to reflux for 2 h and cooled to room temperature. The precipitate formed was collected by filtration and washed by cyclohexane repeatedly. Yield: 35 %; m.p. 217.0–219.0 °C; IR (KBr): $\tilde{\nu} = 3318$ (OH), 1763 and 1732 (ester carbonyl), 1622 cm$^{-1}$ (C=N); elemental analysis (%) calcd for $C_{89}H_{118}N_2O_{10}$: C 77.69, H 8.64, N 2.04; found: C 77.07, H 8.50, N 1.93; $^1$H NMR (300 MHz, TMS, $CDCl_3$): $\delta = 8.60$ (s, 2H), 7.36 (s, 2H), 7.23 (d, $J = 2.4$ Hz, 4H), 6.77 (d, $J = 2.4$ Hz, 4H), 6.72 (d, $J = 2.1$ Hz, 2H), 6.70 (d, $J = 2.1$ Hz, 2H), 5.38 (d, $J = 4.2$ Hz, 2H), 4.68 (m, 2H), 4.04 (s, 2H), 2.87 (t, $J = 7.2$ Hz, 4H), 2.73 (t, $J = 7.2$ Hz, 4H), 2.33 (t, $J = 7.2$ Hz, 4H), 2.20–1.5 ppm (m, 82H).

## Acknowledgements

This work was financially supported by the National Nature Science Foundation of China (NNSFC, 20574027) and the Program for New Century Excellent Talents in University (NCET).

[1] a) P. Terech, R. G. Weiss, *Chem. Rev.* **1997**, *97*, 3133–3159; b) J. H. van Esch, B. L. Feringa, *Angew. Chem.* **2000**, *112* 2351–2354; *Angew. Chem. Int. Ed.* **2000**, *39*, 2263–2266; c) N. M. Sangeetha, U. Maitra, *Chem. Soc. Rev.* **2005**, *34*, 821–836; d) A. Brizard, R. Oda, I. Huc, *Top. Curr. Chem.* **2005**, *256*, 167–218; e) D. J. Abdallah, R. G. Weiss, *Adv. Mater.* **2000**, *12*, 1237–1247; f) R. J. H. Hafkamp, M. C. Feiters, R. J. M. Nolte, *J. Org. Chem.* **1999**, *64*, 412–426.

[2] a) K. Sugiyasu, N. Fujita, S. Shinkai, *Angew. Chem.* **2004**, *116*, 1249–1253; *Angew. Chem. Int. Ed.* **2004**, *43*, 1229–1233; b) T. Nakashima, N. Kimizuka, *Adv. Mater.* **2004**, *14*, 1113–1116.

[3] a) V. K. Praveen, S. J. George, R. Varghese, C. Vijayakumar, A. Ajayaghosh, *J. Am. Chem. Soc.* **2006**, *128*, 7542–7550; b) A. Del Guerzo, A. G. L. Olive, J. Reichwagen, H. Hopf, J.-P. Desvergne, *J. Am. Chem. Soc.* **2005**, *127*, 17984–17985; c) M. Montalti, L. S. Dolci, L. Prodi, N. Zaccheroni, M. C. A. Stuart, K. J. C. van Bommel, A. Friggeri, *Langmuir* **2006**, *22*, 2299–2303; d) D. Beljonne, E. Hennebicq, C. Daniel, L. M. Herz, C. Silva, G. D. Scholes, F. J. M.

  

Hoeben, P. Jonkheijm, A. P. H. J. Schenning, S. C. J. Meskers, R. T. Phillips, R. H. Friend, E. W. Meijer, *J. Phys. Chem. B* **2005**, *109*, 10594–10604; e) J. H. Jung, S. J. Lee, J. A. Rim, H. Lee, T. Bae, S. S. Lee, S. Shinkai, *Chem. Mater.* **2005**, *17*, 459–462; f) T. Sagawa, S. Fukugawa, T. Yamada, H. Ihara, *Langmuir* **2002**, *18*, 7223–7228; g) H. Ihara, T. Yamada, M. Nishihara, T. Sakurai, M. Takafuji, H. Hachisako, T. Sagawa, *J. Mol. Liq.* **2004**, *111*, 73–76.

[4] a) T. Suzuki, S. Shinkai, K. Sada, *Adv. Mater.* **2006**, *18*, 1043–1046; b) S. Yagai, T. Nakajima, K. Kishikawa, S. Kohmoto, T. Karatsu, A. Kitamura, *J. Am. Chem. Soc.* **2005**, *127*, 11134–11139; c) Z. Yang, H. Gu, D. Fu, P. Gao, J. K. Lam, B. Xu, *Adv. Mater.* **2004**, *16*, 1440–1444; d) A. Shumburo, M. C. Biewer, *Chem. Mater.* **2002**, *14*, 3745–3750; e) S. R. Haines, R. G. Harrison, *Chem. Commun.* **2002**, 2846–2847; f) S. Kiyonaka, K. Sugiyasu, S. Shinkai, I. Hamachi, *J. Am. Chem. Soc.* **2002**, *124*, 10954–10955; g) W. Weng, J. B. Beck, A. M. Jamieson, S. J. Rowan, *J. Am. Chem. Soc.* **2006**, *128*, 11663–11672; h) S. Kawano, N. Fujita, S. Shinkai, *J. Am. Chem. Soc.* **2004**, *126*, 8592–8593; i) K. Tsuchiya, Y. Orihara, Y. Kondo, N. Yoshino, T. Ohkubo, H. Sakai, M. Abe, *J. Am. Chem. Soc.* **2004**, *126*, 12282–12283.

[5] a) J. J. D. de Jong, T. D. Tiemersma-Wegman, J. H. van Esch, B. L. Feringa, *J. Am. Chem. Soc.* **2005**, *127*, 13804–13805; b) M. de Loos, J. H. van Esch, R. M. Kellogg, B. L. Feringa, *Angew. Chem.* **2001**, *113*, 633–636; *Angew. Chem. Int. Ed.* **2001**, *40*, 613–616; c) S. Kawano, N. Fujita, S. Shinkai, *Chem. Commun.* **2003**, 1352–1353; d) P. Mukhopadhyay, Y. Iwashita, M, Shirakawa, S. Kawano, N. Fujita, S. Shinkai, *Angew. Chem.* **2006**, *118*, 1622–1625; *Angew. Chem. Int. Ed.* **2006**, *45*, 1592–1595.

[6] a) S. Li, L. He, F. Xiong, Y. Li, G. Yang, *J. Phys. Chem. B* **2004**, *108*, 10887–10892; b) A. Ohshima, A. Momotake, R. Nagahata, T. Arai, *J. Phys. Chem. A* **2006**, *109*, 9731–9736.

[7] a) E. Hadjoudis, M. Vittorakis, I. Moustakali-Mavridis, *Tetrahedron* **1987**, *43*, 1345–1360; b) E. Hadjoudis, *Mol. Eng.* **1995**, *5*, 301–337; c) J. Zhao, B. Zhao, J. Liu, A. Ren, J. Feng, *Chem. Lett.* **2000**, 268–269; d) M. Taneda, K. Amimoto, H. Koyama, T. Kawato, *Org. Biomol. Chem.* **2004**, *2*, 499–504; e) E. Hadjoudis, I. M. Mavridis, *Chem. Soc. Rev.* **2004**, *33*, 579–588; f) K. Ogawa, J. Harada, *J. Mol. Struct.* **2003**, *647*, 211–216.

[8] a) T. Inabe, S. Gautier-Luneau, N. Hoshino, K. Okaniwa, H. Okamoto, T. Mitani, U. Nagashima, Y. Maruyama, *Bull. Chem. Soc. Jpn.* **1991**, *64*, 801–810; b) T. Inabe, I. Luneau, T. Mitani, Y. Maruyama, S. Takeda, *Bull. Chem. Soc. Jpn.* **1994**, *67*, 612–621; c) K. Wozniak, H. He, J. Klinowski, W. Jones, T. Dziembowska, E. Grech, *J. Chem. Soc. Faraday Trans.* **1995**, *91*, 77–85; d) A. R. Katritzky, I. Ghiviriga, P. Leeming, F. Soti, *Magn. Reson. Chem.* **1996**, *34*, 518–526; e) S. H. Alarcón, A. C. Olivieri, A. Nordon, R. K. Harris, *J. Chem. Soc. Perkin Trans. 2* **1996**, 2293–2296; f) T. Sekikawa, T. Kobayashi, T. Inabe, *J. Phys. Chem. A* **1997**, *101*, 644–649; g) K. Ogawa, J. Harada, T. Fujiwara, S. Yoshida, *J. Phys. Chem. A* **2001**, *105*, 3425–3427.

[9] a) A. Ohshima, A. Momotake, T. Arai, *J. Photochem. Photobiol. A* **2004**, *162*, 473–479; b) A. Ohshima, A. Momotake, T. Arai, *Bull. Chem. Soc. Jpn.* **2006**, *79*, 305–311.

[10] a) C. V. Yelamaggad, S. A. Nagamani, U. S. Hiremath, D. S. S. Rao, S. K. Prasad, *Liq. Cryst.* **2002**, *29*, 1401–1408; b) R. Achten, A. Koudijs, Z. Karczmarzyk, A. T. M. Marcelis, E. J. R. Sudhölter, *Liq. Cryst.* **2004**, *31*, 215–227; c) M. Šepelj, A. Lesac, U. Baumeister, S. Diele, D. W. Bruce, Z. Hameršak, *Chem. Mater.* **2006**, *18*, 2050–2058.

[11] K. Nakatani, J. A. Delaire, *Chem. Mater.* **1997**, *9*, 2682–2684.

[12] H. Birkedal, P. Pattison, *Cryst. Struct. Commun.* **2006**, *c62*, o139-o141.

[13] H. Fukuda, K. Amimoto, H. Koyama, T. Kawato, *Org. Biomol. Chem.* **2003**, *1*, 1578–1583.

[14] a) D. J. Abdallah, R. G. Weiss, *Adv. Mater.* **2000**, *12*, 1237–1247; b) M. Zinic, F. Vögtle, F. Fages, *Top. Curr. Chem.* **2005**, *256*, 39–76.

[15] a) R. Wang, C. Geiger, L. H. Chen, B. Swanson, D. G. Whitten, *J. Am. Chem. Soc.* **2000**, *122*, 2399–2400; b) P. C. Xue, R. Lu, D. Li, M. Jin, C. H. Tan, C. Y. Bao, Z. M. Wang, Y. Y. Zhao, *Langmuir* **2004**, *20*, 11234–11239.

[16] a) P. Babu, N. M. Sangeetha, P. Vijaykumar, U. Maitra, K. Rissanen, A. R. Raju, *Chem. Eur. J.* **2003**, *9*, 1922–1932; b) C. Y. Bao, R. Lu, M. Jin, P. C. Xue, C. H. Tan, G. F. Liu, Y. Y. Zhao, *Chem. Eur. J.* **2006**, *12*, 3287–3294.

[17] a) M. Simonyi, Z. Bikádi, F. Zsila, J. Deli, *Chirality* **2003**, *15*, 680–698; b) S. Yagai, M. Higashi, T. Karatsu, A. Kitamura, *Chem. Mater.* **2005**, *17*, 4392–4398.

[18] a) M. Kasha, H. R. Rawls, M. Ashraf El-Bayoumi, *Pure Appl. Chem.* **1965**, *11*, 371–392; b) F. D. Lewis, X. Liu, Y. Wu, X. Zuo, *J. Am. Chem. Soc.* **2003**, *125*, 12729–12731; c) P. C. Xue, R. Lu, Y. Huang, M. Jin, C. H. Tan, C. Y. Bao, Z. M. Wang, Y. Y. Zhao, *Langmuir* **2004**, *20*, 6470–6475; d) F. D. Lewis, L. Zhang, X. Liu, X. Zuo, D. M. Tiede, H. Long, G. C. Schatz, *J. Am. Chem. Soc.* **2005**, *127*, 14445–14453.

[19] F. Würthner, Z. Chen, F. J. M. Hoeben, P. Osswald, C. You, P. Jonkheijm, J. v. Herrikhuyzen, A. P. H. J. Schenning, P. P. A. M. van der Schoot, E. W. Meijer, E. H. A. Beckers, S. C. J. Meskers, R. A. J. Janssen, *J. Am. Chem. Soc.* **2004**, *126*, 10611–10618.

[20] C. Thalacker, F. Würthner, *Adv. Funct. Mater.* **2002**, *12*, 209–218.

[21] A. Ajayaghosh, C. Vijayakumar, R. Varghese, S. J. George, *Angew. Chem.* **2006**, *118*, 470–474; *Angew. Chem. Int. Ed.* **2006**, *45*, 456–460.

[22] a) D. C. Duncan, D. G. Whitten, *Langmuir* **2000**, *16*, 6445–6452; b) J. Makarević, M. Jokić, Z. Raza, Z. Štefanić, B. Kojić-Prodić, M. Žinić, *Chem. Eur. J.* **2003**, *9*, 5567–5580; c) M. Ikeda, T. Nobori, L. M. J. Schmutz, *Chem. Eur. J.* **2005**, *11*, 662–668; d) S. J. George, A. Ajayaghosh, *Chem. Eur. J.* **2005**, *11*, 3217–3227.

[23] M. Tata, V. T. John, Y. Y. Waguespack, G. L. McPherson, *J. Am. Chem. Soc.* **1994**, *116*, 9464–9470.

[24] A. G. J. Ligtenbarg, R. Hage, A. Meetsmaa, B. L. Feringa, *J. Chem. Soc. Perkin Trans. 2* **1999**, 807–812.

[25] a) M. George, R. G. Weiss, *Chem. Mater. 2003, 15*, 2879–2888; b) Y. Zhou, T. Yi, T. Li, Z. Zhou, F. Li, W. Huang, C. Huang, *Chem. Mater.* **2006**, *18*, 2974–2981.

[26] T. Sekikawa, T. Kobayashi, T. Inabe, *J. Phys. Chem. A* **1997**, *101*, 644–649.

[27] J. Luo, Z. Xie, J. W. Y. Lam, L. Cheng, H. Chen, C. Qiu, H. S. Kwok, X. Zhan, Y. Liu, D. Zhu, B. Tang, *Chem. Commun.* **2001**, 1740–1741.

[28] S. Kim, Q. Zheng, G. S. He, D. J. Bharali, H. E. Pudavar, A. Baev, P. N. Prasad, *Adv. Funct. Mater.* **2006**, *16*, 2317–2323.

[29] C. Y. Bao, R. Lu, M. Jin, P. C. Xue, C. H. Tan, G. F. Liu, Y. Y. Zhao, *Org. Biomol. Chem.* **2005**, *3*, 2508–2512.

[30] B. An, S. Kwon, S. Jung, S. Y. Park, *J. Am. Chem. Soc.* **2002**, *124*, 14410–14415.

[31] A. Chowdhury, S. Wachsmann-Hogiu, P. R. Bangal, I. Raheem, L. A. Peteanu, *J. Phys. Chem. B* **2001**, *105*, 12196–12201.

[32] a) K. Ogawa, Y. Kasahara, Y. Ohtani, J. Harada, *J. Am. Chem. Soc.* **1998**, *120*, 7107–7108; b) J. Harada, H. Uekusa, Y. Ohashi, *J. Am. Chem. Soc.* **1999**, *121*, 5809–5810.

[33] K. Amimoto, H. Kanatomi, A. Nagakari, H. Fukuda, H. Koyama, T. Kawato, *Chem. Commun.* **2003**, 870–871.

[34] The supporting information for this article contains the UV/Vis spectra of **1′** in dilute solution and the crystal state, the FT-IR spectra of the xerogel before and after irradiation, and the TEM image of the benzene/cyclohexane gel.

[35] Y. Q. Tian, X. H. Xu, Y. Y. Zhao, X. Y. Tang, T. J. Li, *Liq. Cryst.* **1997**, *22*, 87–96.

Received: February 27, 2007
Published online: July 23, 2007

  